

Interaction of porous germanium structure with incoherent light pulses

A. L. STEPANOV^{1,*}, YA. V. FATTAKHOV¹, A. M. ROGOV^{1,2}, D. A. KONOVALOV¹, B. F. FARRAKHOV¹, V. I. NUZHIDIN¹, V. F. VALEEV¹

¹Zavoisky Physical-Technical Institute, FRC Kazan Scientific Center of RAS, 420029, Kazan, Russia

²Kazan Federal University, 420008, Kazan, Russia

The paper addresses the study of monocrystalline *c*-Ge wafers implanted by Ag⁺ ions at current density $J=5 \mu\text{A}/\text{cm}^2$, dose $D=2.5 \cdot 10^{16} \text{ ion}/\text{cm}^2$, energy 30 keV and subjected to rapid thermal processing annealing with single light pulses of various duration from 1 to 9.5 s. It was found that annealing with an increasing pulse duration to 5 s consequently led to growing diameters of Ge nanowires from 26 to 35 nm, which constitute an amorphous sponge-like structure of Ag:PGe with nanowires formed by ion implantation. It was assumed that increase in the nanowire diameters occurred by the mechanism of Ostwald ripening in the samples heated during the annealing. Annealing with the pulses exceeding 5 s caused the porous structure destruction and Ag evaporation in the samples. Partial recrystallization of the implanted Ag:PGe layers annealed by incoherent light pulses with duration of more than 1 s was observed.

(Received May 16, 2023; accepted December 4, 2023)

Keywords: Ion implantation, Nanoporous germanium, Incoherent-light pulse annealing

1. Introduction

At present, for fast and efficient modification of the structure and properties of various ion-implanted semiconductor materials, the annealing technologies by light pulses of different duration (τ) are widely used. The following technologies differ in τ : (1) pulsed laser annealing with $\tau = 1 - 1000 \text{ ns}$; (2) flash lamp annealing (FLA) with $\tau = 100 \mu\text{s} - 100 \text{ ms}$ and (3) rapid thermal processing (RTP) performed by halogen lamps at significantly higher $\tau = 1 - 100 \text{ s}$ [1]. The main difference between these technologies in the effect on the semiconductor material is the depth of heating and modification of the surface layer. In case of RTP, the greatest depth is reached.

Thin layers of nanoporous germanium (PGe) formed by ion implantation present interesting objects annealed by pulses of incoherent light [2]. In the work [2], by the implantation of heavy $^{119}\text{Sn}^+$ ions into monocrystalline *c*-Ge wafers at energy $E = 150 \text{ keV}$, current density $J = 0.35 \mu\text{A}/\text{cm}^2$, and doses $D = 1.4 \cdot 10^{15} - 4.2 \cdot 10^{15} \text{ ion}/\text{cm}^2$ Sn:PGe layers with open pores of the honeycomb structure with thickness 300 nm were formed. These Sn:PGe layers were used to study the possibilities of FLA with $\tau = 3 \text{ ms}$. According to Raman spectroscopy data, the annealed samples are crystalline and Sn is incorporated into the Ge lattice [2], forming the GeSn alloy [3]. At the same time, it was suggested that the observed recrystallization of the implanted layer occurred due to the solid phase epitaxy. Generally, the Sn:PGe honeycomb structure was retained after FLA, although some destruction or melting was observed in local places on the sample surface. This work presents the experimental

results on RTP annealing by light pulses with various τ of Ag:PGe layers with a morphological porous surface formed by the low-energy high-dose implantation with Ag⁺ ions [4, 5].

2. Experimental

Polished *c*-Ge wafers with *n*-type conductivity, 0.5 mm thickness and crystallographic orientation (111) were used as substrates for the ion implantation. Implantation was carried out with Ag⁺ ions with $E = 30 \text{ keV}$, $D = 2.5 \cdot 10^{16} \text{ ion}/\text{cm}^2$ at $J = 5 \mu\text{A}/\text{cm}^2$ using ILU-3 ion accelerator at a normal angle of incidence of the ion beam on the *c*-Ge surface. RTP annealing of implanted Ag:PGe samples was performed out by Impulse-6 setup with a sealed reaction chamber where halogen lamps are used as heating elements. The light exposure was carried out by a single pulse with a different value $\tau = 1-9.5 \text{ s}$. Sample temperature was controlled using a thermocouple, and the shape of the light pulse was monitored by a photodiode. Fig. 1 shows the diagrams of the temperature variation of implanted Ag:PGe samples with time during RTP annealing. The maximum temperature values of the samples ($T = 250-950 \text{ }^\circ\text{C}$) corresponding to pulses with different τ are also presented in Fig. 1. The diagrams demonstrate the inhomogeneous dynamics of heating the samples. For the shortest light exposure with $\tau = 1 \text{ s}$, there is a sharp increase in temperature to $T = 250 \text{ }^\circ\text{C}$ with a rapid decrease after the termination of the light pulse. For light pulses with greater τ a continuous monotonic increase and a gradual decrease of the sample temperature are observed. For the description of the experimental

results, the samples were designated in the article by the maximum temperature attained during RTP annealing: 250, 400, 520, 770, and 950 °C. The study of the surface morphology of the samples and elemental chemical analysis energy dispersive (EDX) analysis were carried

out by scanning electron microscope (SEM) Merlin (Carl Zeiss) with X-Max spectrometer (Oxford Instruments). Optical reflection spectra were collected with an AvaSpec-2048 (Avantes) spectrometer in the spectral diapason 220 - 1100 nm.

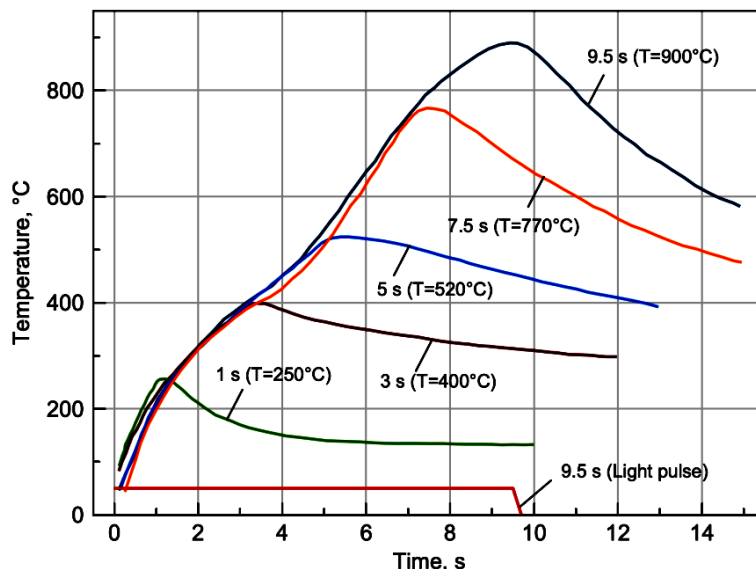


Fig. 1. Diagrams of temperature variation of implanted Ag:PGe samples with time during RTP annealing for light pulses with different τ . The maximum temperature values for each τ are indicated in parentheses. As an example, the light pulse shape with $\tau = 9.5$ s measured by a photodiode is shown (color online)

3. Results and discussion

The SEM image of the Ag:PGe sample surface formed by implantation with Ag^+ ions and the histogram of the size distribution of Ge nanowire \varnothing are shown in

Fig. 2. The SEM image seems similar to the sponge-like structures observed earlier in the works [4, 5]. As seen from the figure, for the chosen ion implantation conditions the value of \varnothing is 26 nm.

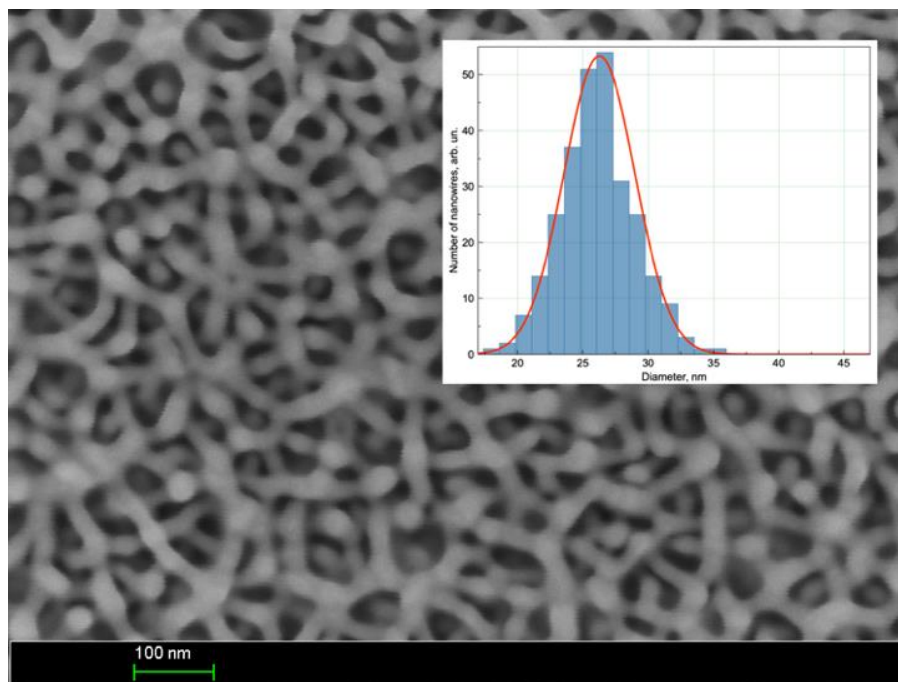


Fig. 2. SEM-image of the Ag:PGe sample surface formed by implantation with Ag^+ ions at $E = 30$ keV, $J = 5 \mu\text{A}/\text{cm}^2$ and $D = 2.5 \cdot 10^{16}$ ion/ cm^2 . The inset shows a histogram of the size distribution of Ge nanowire \varnothing (color online)

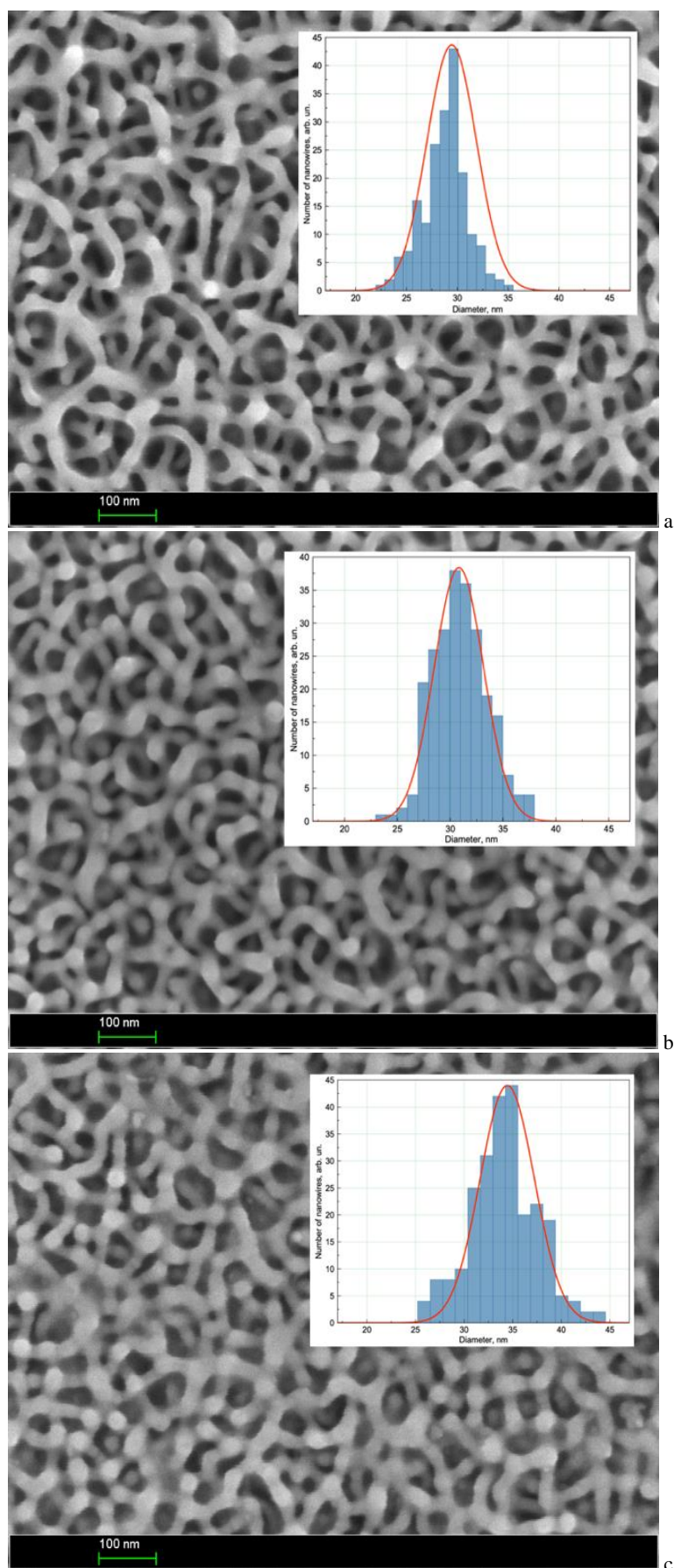


Fig. 3. SEM-images of Ag:PGe sample surfaces after RTP annealing by light pulses with different values of τ : (a) 1 ($T = 250^\circ\text{C}$); (b) 3 ($T = 400^\circ\text{C}$) and (c) 5 ($T = 520^\circ\text{C}$) s. The inset shows a histogram of the size distribution of Ge nanowire \varnothing (color online)

Fig. 3 presents SEM images of Ag:PGe layers after RTP annealing by light pulses with $\tau = 1, 3,$ and 5 s, which caused heating of the samples to $T = 250, 400,$ and 520 °C respectively. All samples demonstrate a spongy-like structure. Monotonic increase of Ge nanowire $\varnothing = 29, 31,$ and 35 nm in the annealed samples is observed simultaneously with an increase in their temperature.

It could be suggested that the mechanism of \varnothing change with increasing Ag:PGe sample temperature may be due to Ostwald ripening [6]. This is facilitated by a decrease in the melting temperature of nanostructured Ge relative to the value of the bulk material $T_{Ge} = 938.25$ °C with a decrease in the dimension of its structure. For example, in the work [7], it was experimentally shown that the melting temperature of Ge nanoparticles with a size of 20 nm is 498 °C. Therefore, during RTP heating of the Ag:PGe layer the thinnest nanowires will be melted and the freed Ge atoms released in this case diffuse and integrate into the sponge-like structure of unbroken nanowires with increasing their \varnothing .

Observed dynamics of a nanowire \varnothing increase when the sample temperature grew during RTP annealing (Fig. 3) qualitatively confirmed the mechanism of Ostwald ripening, since at higher temperatures a larger number of nanowires are expected to be melting, including those with

bigger \varnothing . However, as follows from Fig. 4, using a light pulse with τ more than 5 s and, accordingly, an increase in the sample temperature above $T = 520$ °C (Fig. 3) complete melting of the spongy-like porous structure occurs. The SEM-image in Fig. 4a demonstrates that after RTP annealing at $\tau = 7.5$ s and reaching the sample temperature $T = 770$ °C the spongy-like Ag:PGe layer on *c*-Ge wafers is absent. The surface of the sample consists of alternating micron-sized regions similar to the smooth surface of *c*-Ge surrounded by ragged melted terraces. Annealing by a light pulse with $\tau = 9.5$ s heats the sample to a temperature of $T = 900$ °C, comparable to the melting temperature T_{Ge} of the bulk material, also leads to the appearance of melted terraces on the sample surface (Fig. 4b). However, the SEM-image of the same sample with a lower magnification (Fig. 4c) additionally shows that as a result of heating and melting of the porous layer some spherical particles up to 5 μ m in size randomly distributed over the surface are formed over the terraces. Composite materials containing Ge spherical particles with a high value of the refractive index are emerging as a promising alternative to plasmonic nanostructures for photonics applications with specific interference effects, scattering anisotropy and strong electromagnetic forces [8, 9].

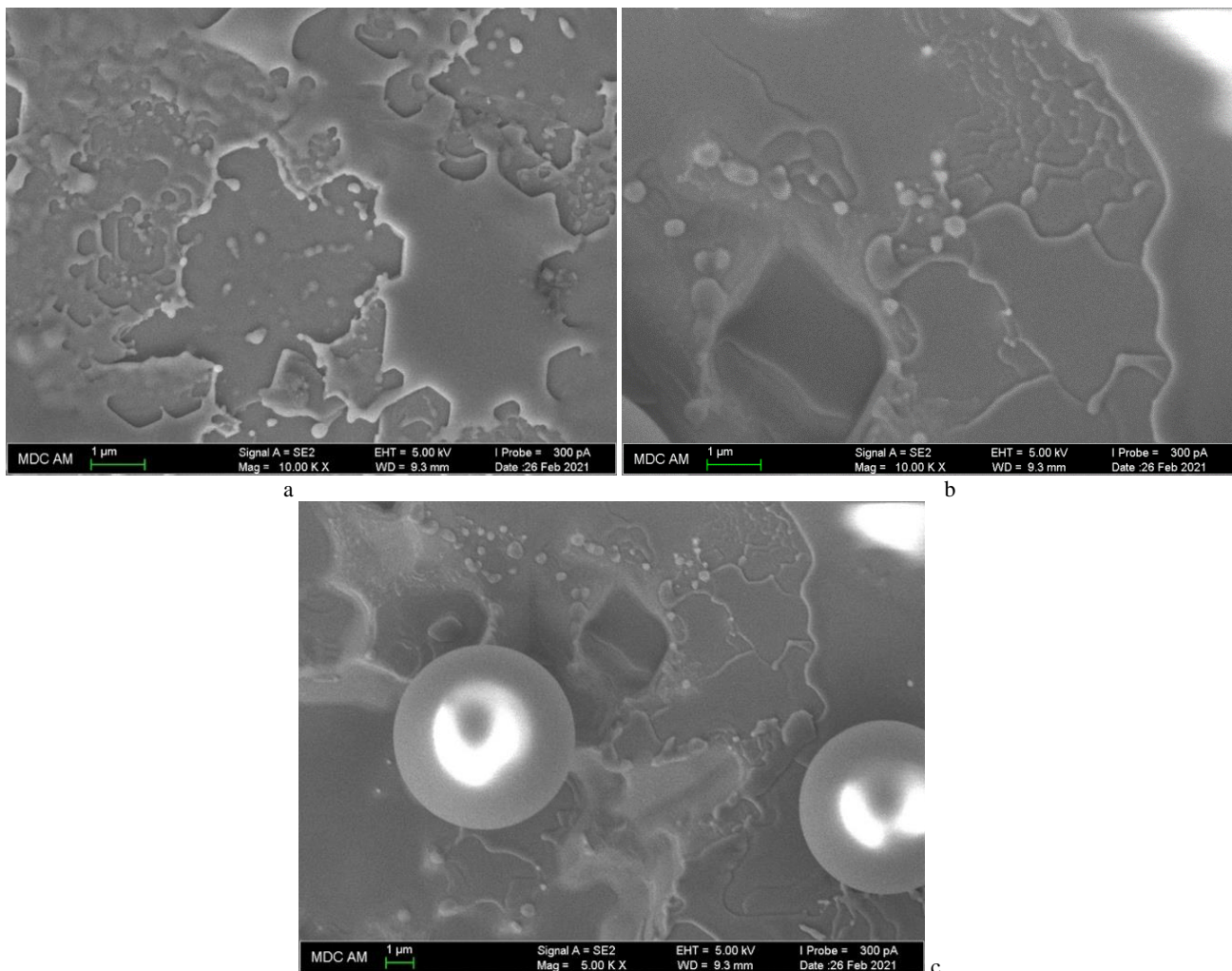


Fig. 4. SEM images of Ag:PGe sample surfaces after RTP annealing by light pulses with different values of τ : (a) 7.5 ($T = 770$ °C); (b and c) 9.5 ($T = 900$ °C) s. Micrograph (c) corresponds to a large-scale SEM image

The EDX measurements of implanted Ag:PGe sample indicate the presence of lines in the spectrum near 2.5 keV corresponding to Ag. After RTP annealing with $\tau = 1, 3,$ and 5 s Ag peaks are also present in the EDX spectra. However, using light pulses with higher values of τ Ag signal is not recorded in the annealed samples. This indicates that at high temperatures in addition to the melting process an intensive evaporation of doping atoms from the surface of heated samples will be stimulated, which leads to the loss of implanted Ag.

Fig. 5 shows the optical reflection spectra from the *c*-Ge substrate, the Ag:PGe sample formed by ion implantation and also the same sample surface after RTP annealing by light pulses with different τ . The spectrum of unimplanted *c*-Ge consists of several bands with maxima at about 276, 564, and 820 nm corresponding to intraband and interband electronic transitions. The intensity of the 276 nm band characterizes the degree of the semiconductor material crystallinity [10–12].

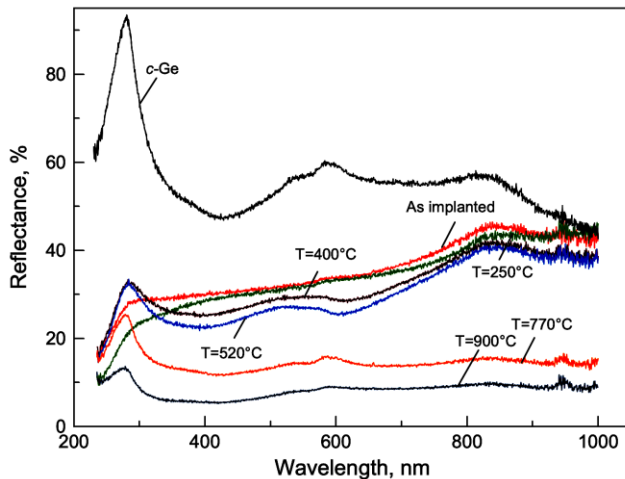


Fig. 5. Optical reflectance spectra of virgin *c*-Ge wafer, implanted and RTP annealed Ag:PGe samples (color online)

Implantation of the *c*-Ge substrate with Ag⁺ ions leads to a strong decrease in the intensity of the reflection bands with maxima at 276 and 564 nm (Fig. 5). This indicates amorphization of the implanted layer and the formation of Ag:PGe structure as it was previously studied in detail in the work [13]. The effect of the reflection intensity decreases with amorphization of the *c*-Ge surface after implantation with Ni⁺ and O⁺ ions was also discovered in the works [12] and [14] respectively. The darkening of the sample, which referred to in the literature as “black Ge,” arises due to increase in Rayleigh light scattering by the nanoporous Ag:PGe structure also causes a decrease of optical reflection intensity [15].

RTP annealing ($\tau = 1$ s, $T = 250$ °C) of the Ag:PGe sample produces the optical reflection intensity decrease in the near-ultraviolet region relative to the implanted material, while in the other part of the optical range the shapes of the spectral bands practically coincide. It could be assumed that the observed decrease in reflection is due to increased Rayleigh light scattering [13], since Ge

nanowires \varnothing increased from 26 to 29 nm (Figs. 2 and 3a). However, during RTP annealing of Ag:PGe sample at $\tau = 3$ s, $T = 400$ °C and $\tau = 5$ s, $T = 520$ °C in contrast to spectrum for $T = 250$ °C there the increase in the intensity of the band is observed with a maximum at 276 nm by about 10%. Despite the increase Ge nanowire \varnothing to 35 nm (Fig. 3c) and the accompanying growth of Rayleigh scattering the effect of partial crystallization of the amorphous implanted Ag:PGe layer prevails. It was also shown in the publications [16, 17] that amorphous layers consisting of Ge nanowires fabricated by the electrochemical method, which were heated by He-Ne laser during the Raman measurement, a partial Ge recrystallization were demonstrated.

During RTP annealing ($\tau = 7.5$ s, $T = 770$ °C; $\tau = 9.5$ s, $T = 900$ °C) of the Ag:PGe sample the reflectance spectra correspond to surfaces without Ge nanowires (Fig. 4), but containing micron terraced formations. Such large formations lead to a shift of the Rayleigh light scattering spectrum from the ultraviolet to the long-wavelength region of the optical range. These low-intensity reflectance wavelength dependencies were close to the spectra of antireflection structures produced on the Ge surface by electrochemical methods [15]. The presence of the band with a maximum at 276 nm also indicates that at such high annealing temperatures the process of partial recrystallization of the implanted layer occurs.

4. Conclusion

Thus, the work discusses the experimental study of *c*-Ge substrates implanted with Ag⁺ ions and subjected to RTP annealing. It was shown that as a result of ion implantation an amorphous porous Ag:PGe layer of spongy structure with nanowires is formed on the *c*-Ge surface. Annealing with an increase in τ from 1 to 5 s leads to an increase in the diameters of Ge nanowires from 26 to 35 nm, which constitutes a sponge-like structure of Ag:PGe. After annealing with τ for more than 5 s the destruction of the porous structure of Ag:PGe and the evaporation of Ag from the samples were observed. For RTP treatment with $\tau = 3$ -9.5 a partial recrystallization of amorphous implanted Ag:PGe occurs. Rapid RTP annealing, which offers an advantage over equilibrium thermal annealing, indicates the practical efficiency of this method for industrial use with porous semiconductor materials.

Acknowledgements

This work was supported by Russian Scientific Foundation, grant No. 19-79-10216 and by the Ministry of Science and Higher Education of the Russian Federation for FRC Kazan Scientific Center of RAS.

References

- [1] S. Prucnal, L. Rebohle, W. Skorupa, *Mater. Sci. Semicond. Processing* **62**, 115 (2017).
- [2] S. Prucnal, J. Zuk, R. Hübner, J. Duan, M. Wang, K. Pyszniak, A. Drozdziel, M. Turek, S. Zhou, *Materials* **13**, 1408 (2020).
- [3] N. Bhargava, M. Coppinger, J. P. Gupta, L. Wielunski, J. Kolodzey, *Appl. Phys. Lett.* **103**, 41908 (2013).
- [4] A. L. Stepanov, V. I. Nuzhdin, V. F. Valeev, A. M. Rogov, V. V. Vorobev, *Vacuum* **152**, 200 (2018).
- [5] A. M. Rogov, A. I. Gumarov, L. R. Tagirov, A. L. Stepanov, *Composit. Comm.* **16**, 57 (2019).
- [6] P. W. Voorhees, *J. Statistical Phys.* **38**, 231 (1985).
- [7] A. F. Lopeandía, J. Rodríguez-Viejo, *Thermochemica Acta* **461**, 82 (2007).
- [8] R. Gómez-Medina, B. García-Cámara, I. Suárez-Lacalle, F. González, F. Moreno, M. Nieto-Vesperinas, J. J. Sáenz, *J. Nanophotonics* **5**, 52512 (2011).
- [9] C. Ma, J. Yan, Y. Huang, G. Yang, *Adv. Opt. Mater.* **5**, 1700761 (2017).
- [10] T. M. Donovan, W. E. Spicer, J. M. Bennett, E. J. Ashley, *Phys. Rev. B* **2**, 397 (1970).
- [11] H. Liu, S. Li, P. Sun, X. Yang, D. Liu, Y. Ji, F. Zhang, D. Chen, Y. Cui, *Mater. Sci. Semicond. Processing* **83**, 58 (2018).
- [12] K. L. Bhatia, P. Singh, M. Singh, N. Kishore, N. C. Mehra, D. Kanjilal, *Nucl. Instr. Meth. Phys. Res. B* **94**, 379 (1994).
- [13] A. L. Stepanov, A. M. Rogov, *Opt. Commun.* **474**, 126052 (2020).
- [14] Q.-C. Zhang, J. C. Kelly, M. J. Kenny, *Nucl. Instr. Meth. Phys. Res. B* **47**, 257 (1990).
- [15] S. Schicho, A. Jaouad, C. Sellmer, D. Morris, V. Aimez, R. Arès, *Mater. Lett.* **94**, 86 (2013).
- [16] A. V. Pavlikov, A. M. Rogov, A. M. Sharafutdinova, A. L. Stepanov, *Vacuum* **184**, 109881 (2021).
- [17] S. A. Gavrilov, A. A. Dronov, I. M. Gavrilin, R. L. Volkov, N. I. Borgardt, A. Y. Trifonov, A. V. Pavlikov, P. A. Forsh, P. K. Kashkarov, *Raman Spectr.* **49**, 810 (2018).

*Corresponding author: aanstep@gmail.com